$Ca(SCN)_2$ and $Ca(SCN)_2 \cdot 2\,H_2O$: Crystal Structure, Thermal Behavior and Vibrational Spectroscopy

Claudia Wickleder and Patrick Larsen

Institut für Anorganische Chemie, Universität zu Köln, Greinstrasse 6, D-50939 Köln, Germany

Reprint requests to Dr. Claudia Wickleder Fax: +49 (0)221 470 5083.
E-mail: claudia.wickleder@uni-koeln.de

Dedicated to Professor Albrecht Mewis on the occasion of his 60th birthday

Z. Naturforsch. **57 b,** 1419–1426 (2002); received September 6, 2002

Thiocyanates, Vibrational Spectroscopy, Hydrogen Bonds

The dehydration of $Ca(SCN)_2{\cdot}4H_2O$ yields single crystals of $Ca(SCN)_2 \cdot 2\,H_2O$ as well as of $Ca(SCN)_2$. $Ca(SCN)_2 \cdot 2\,H_2O$ crystallizes with a hitherto unknown structure (orthorhombic, *Pnma*, $Z = 4$, $a = 1280.1(2)$, $b = 790.3(1)$, $c = 726.9(1)$ pm, $R_{\text{all}} = 0.0430$). The Ca^{2+} ions are surrounded by four SCN^- ions and four water molecules. The polyhedra are connected to chains along [010] via common oxygen atoms. The SCN^- ions connect these chains to a three-dimensional network so that each thiocyanate group is linked to two Ca^{2+} ions. Hydrogen bonding with sulfur atoms as acceptors is observed. The crystal structure of $Ca(SCN)_2$ (monoclinic, *C2/c*, $Z = 4$, $a = 961.7(2)$, $b = 642.4(2)$, $c = 787.2(2)$ pm, $R_{\text{all}} = 0.0673$) consists of alternating layers of Ca^{2+} and SCN^- ions. The cations are surrounded by four sulfur and four nitrogen atoms in form of a square antiprism. According to ${}^3_\infty[Ca(SCN)_{8/4}]$ each SCN^- ion connects four Ca^{2+} ions with each other. Thermal investigations show a phase transition of $Ca(SCN)_2 \cdot 4\,H_2O$ followed by dehydration to $Ca(SCN)_2$ which finally decomposes yielding CaS. IR and Raman measurements have been performed and the resulting frequencies assigned and discussed.

Introduction

Due to its strong parity allowed electronic transitions, the luminescence of Eu^{2+} ions is used in several applications, like tricolour lamps and X-ray storage phosphors [1]. In this case the energy of the luminescence, *e. g.* the position of the opposite parity $4f^5 5d^1$ state, depends very strongly on the host lattice. Above all, the wavelength of the emission is determined by the nature of the ligands. There are many investigations on the optical properties of divalent europium in oxide and halide host lattices where mostly an emission in the blue or ultraviolet range is observed [2]. Investigations of other host lattices like chalcogenides are very scarce although a red shifted emission can be expected bearing potential for several new applications.

Recently, we started to investigate solvent free "binary" earth alkaline thiocyanates, $M(SCN)_2$ (M = Sr, Ba), in view of their properties as host lattices [3]. Fortunately, $Eu(SCN)_2$ turned out to be isotypic [3] so that doping experiments can be easily carried out. Main feature of the crystal structure is the coordination of the M^{2+} ions with four sulfur and just as many nitrogen atoms in form of a square antiprism. The unusual surrounding causes a quite uncommon and very intense green emission of the Eu^{2+} doped thiocyanates $M(SCN)_2$ (M = Sr, Ba) at low temperatures [4]. In order to shift the $4f^5 5d^1 \rightarrow 4f^6$ emission to even lower energy we considered $Ca(SCN)_2$ to be an appropriate host lattice. Unfortunately, structural data are not available up to now. On the other hand the tetrahydrate $Ca(SCN)_2 \cdot 4\,H_2O$ has been characterized previously [5] and was thought to be an appropriate starting material to prepare the anhydrous compounds by dehydration. Indeed, $Ca(SCN)_2$ can be pepared in this way, even in single crystalline form. Furthermore, we were able to obtain a dihydrate as an intermediate of the dehydration reaction and to determine its crystal structure. Thus, in the present paper we present the crystal structures, the thermal behavior and the vibrational spectroscopy of the two calcium thiocyanates $Ca(SCN)_2 \cdot 2\,H_2O$ and $Ca(SCN)_2$.

Table 1. Crystallographic data of $Ca(SCN)_2 \cdot 2\ H_2O$ and $Ca(SCN)_2$ and their determination.

Compound	$Ca(SCN)_2 \cdot 2\ H_2O$	$Ca(SCN)_2$
Lattice parameter	a = 1280.1(2) pm b = 790.3(1) pm c = 726.9(1) pm β = 90.82(3)°	a = 961.7(2) pm b = 642.4(2) pm c = 787.2(2) pm
Molar volume	110.74 cm^3/mol	73.22 cm^3/mol
No. of formula units	4	4
Crystal system	orthorhombic	monoclinic
Space group	*Pnma* (No. 62)	*C2/c* (no. 15)
Measuring device	Stoe IPDS I	Stoe IPDS I
Radiation	Mo-K_α (graphite monochrom., λ = 71.07 pm)	
Temperature	20 °C	20 °C
Theta range	$2° < 2\theta < 50°$	$5° < 2\theta < 56°$
Rotation angle; φ increment	$0° < \varphi < 200°$; 2°	$0° < \varphi < 200°$; 2°
Index range	$-16 \leq h \leq 16, -10 \leq k \leq 10,$ $-9 \leq l \leq 9$	$-12 \leq h \leq 12, -8 \leq k \leq 8,$ $-10 \leq l \leq 10$
No. of exposures	100	100
Exposure time	4 min	5 min
Detector distance	60	60
Absorption correction	numerical after crystal shape optimisation [8]	
μ	13.51 cm^{-1}	19.88 cm^{-1}
Measured reflections	5939	2242
Unique reflections	653	598
— with $I_o > 2\sigma(I)$	498	409
No. of variables	60	33
R_{int}	0.1382	0.0644
Structure determinations	SHELXS-86 und SHELXL-93 [7]	
Scattering factors	Intern. Tables, Vol. C [9]	
Goodness of fit	0.933	0.888
$R1$; $wR2$ ($I_o > 2\sigma(I)$)	0.0277; 0.0531	0.0323; 0.0540
$R1$; $wR2$ (all data)	0.0430; 0.0556	0.0637; 0.0612
CSD no.	412784	412783

Table 2. Atomic positions and equivalent isotropic displacement parameters (in pm^2) for $Ca(SCN)_2 \cdot 2\ H_2O$.

Atom	Site	*x/a*	*y/b*	*z/c*	$U_{eq} \cdot 10^{-1}$
Ca	4*c*	0.95583(6)	1/4	0.04386(9)	17.7(2)
S1	4*c*	0.72077(7)	1/4	0.9146(1)	25.5(3)
C1	4*c*	0.6356(3)	1/4	0.0841(5)	27.6(9)
N1	4*c*	0.0769(3)	1/4	0.2941(5)	46(1)
S2	4*c*	0.81755(8)	1/4	0.3906(1)	28.1(3)
C2	4*c*	0.8898(3)	1/4	0.5778(5)	26.8(9)
N2	4*c*	0.9369(3)	1/4	0.7140(4)	40.7(9)
O	8*d*	0.8978(2)	0.9500(2)	0.0663(3)	22.3(4)
H1	8*d*	0.884(2)	0.933(3)	0.159(5)	21(9)
H2	8*d*	0.845(3)	0.937(4)	0.019(5)	47(11)

$U_{eq} = {}^1/_3[U_{11} + U_{22} + U_{33}]$ [10].

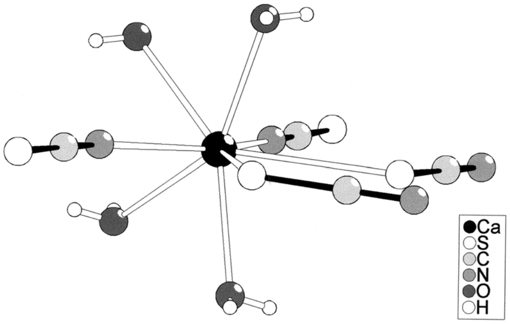

Fig. 1. $[Ca(SCN)_4(H_2O)_4]$ polyhedron in the crystal structure of $Ca(SCN)_2 \cdot 2\ H_2O$.

Experimental Section

$Ca(SCN)_2 \cdot 4\ H_2O$ was obtained by mixing a slurry of 100 g of $Ca(OH)_2$ (p. a., Merck) in about 500 ml of H_2O and a stock solution of NH_4SCN. The mixture was stirred for 2 - 3 d at 50 °C. To avoid the formation of unsoluble $CaCO_3$, attention had to be paid that no CO_2 from air can contaminate the solution. Upon slow evaporation at 50 °C the tetrahydrate started to precipitate. The evaporation must not be continued to dryness in order to avoid formation of lower hydrates. Instead, the precipitate is to be filtered off. If the evaporation is carried out at 90 °C, samples of the dihydrate, $Ca(SCN)_2 \cdot 2\ H_2O$, could be obtained in pure phases according to X-ray pow-

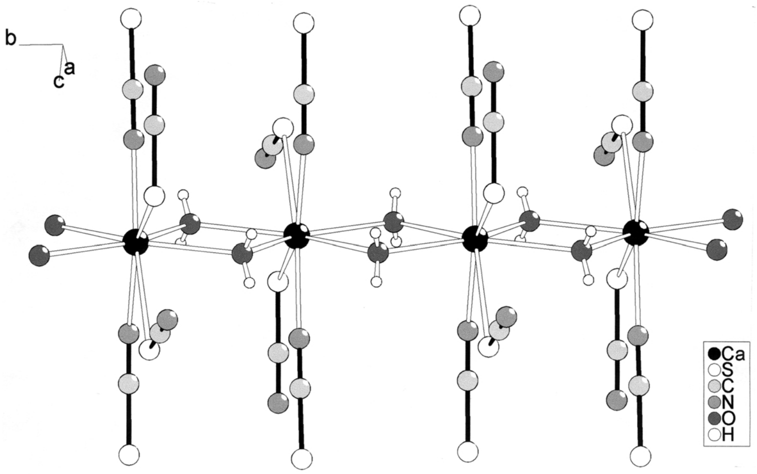

Fig. 2. $^{1}_{\infty}[Ca(SCN)_{4/1}(H_2O)_{4/2}]$ chain along [010] in the crystal structure of $Ca(SCN)_2 \cdot 2\,H_2O$.

der diffraction measurements (Stoe, Stadi P). The very hygroscopic solid contained colorless prismatic single crystals.

In contrast to statements that it is not possible to dry $Ca(SCN)_2{\cdot}2H_2O$ without decomposition [6], pure samples of $Ca(SCN)_2$ could be obtained by heating the dihydrate in a vacuum to 300 °C for 5 d. During this procedure some small colorless cube shaped single crystals formed. The sample is hygroscopic and must be handled in an argon box.

Some crystals of the two compounds were selected using a polarizing microscope and then sealed in glass capillaries (d = 0.1 mm). To check their quality, several exposures were taken with an image plate X-ray diffractometer (STOE IPDS I), which was also used to collect diffraction data of the best specimen. The structure was solved and refined using the programs SHELXS-86 and SHELXL-93 [7], respectively. For $Ca(SCN)_2 \cdot 2\,H_2O$ the position of the hydrogen atoms were taken from the difference Fourier map and refined isotropically. Absorption corrections were applied to the data with the help of the programs X-red and X-shape [8]. Crystallographic details are summarized in the Tables 1 - 3 and are available from the Fachinformationszentrum Karlsruhe, D-76344 Eggenstein-Leopoldshafen (crysdata@FIZ-Karlsruhe.de) on quoting the deposition number given in Table 1.

DTA/TG investigations were performed using a STA 409 thermal analyzer (Netzsch). For that purpose about 20 mg of $Ca(SCN)_2 \cdot 4\,H_2O$ were filled in corundum containers and heated at a constant rate of 10 K/min under flowing argon. The thermal behavior was monitored from 30 °C up to 800 °C. For the DTA data a baseline correction was applied. Onset and end temperatures of the thermal effects were taken from the differentiated DTA curve following common procedures using the software supplied with the analyzer [11].

For temperature dependent powder diffraction investigations about 100 mg of $Ca(SCN)_2 \cdot 2\,H_2O$ was placed on a silver plate under flowing argon in a heatable chamber (Bühler, HDK 2.4). Data were collected by a powder θ/θ diffractometer (Stoe, Stadi P) in the range of $2\,\theta = 7° - 60°$ between 30 and 600 °C with a 20 °C step width.

IR and Raman spectra were recorded using an FTIR spectrometer (Bruker, IFS 66v/S) with a Raman equipment (Bruker, FRA 166/S) and a resolution of 2 cm^{-1}. For excitation, the 1064 nm line of a Nd:YAG laser was employed. For IR measurements the samples were mixed with dry KBr and pressed to a pellet while for Raman investigations pure samples melted in glass tubes were used.

Results and Discussion

Crystal structure

$Ca(SCN)_2 \cdot 2\,H_2O$ crystallizes with a hitherto unkown structure with the orthorhombic space group *Pnma* and four formula units per unit cell (Table 1). There is only one crystallographically independent Ca^{2+} ion (Table 2) which is surrounded by four water molecules and four thiocyanate ions in form of a distorted square antiprism (Fig. 1). Two oxygen, one sulfur and one nitrogen atom belong to each square plane. The two crystallographically different SCN^- ions within each coordination sphere are either connected *via* the terminal sulfur or via the terminal nitrogen atoms to the cations. There are two different Ca-S (308 and 315 pm) and Ca-N (239 and 241 pm) distances. The latter are comparable to those in $Ca(SCN)_2 \cdot 4\,H_2O$ [5] (245 pm) while there are no Ca-S contacts in the tetrahydrate. The

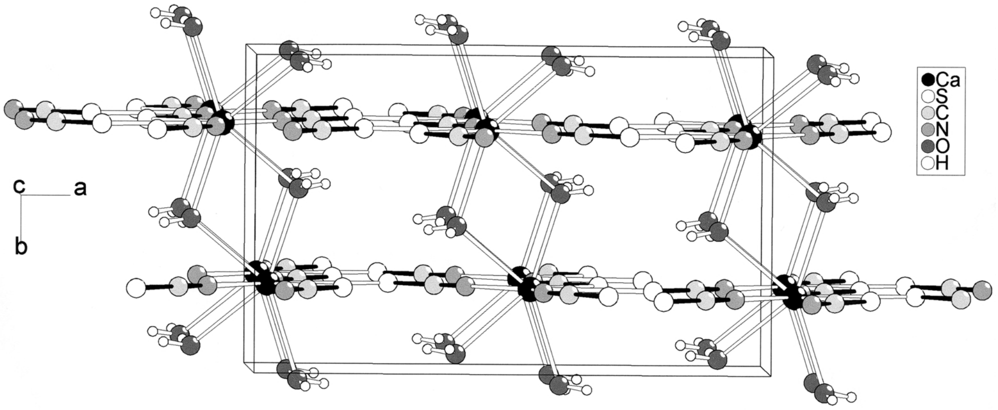

Fig. 3. Perspective *view* of the crystal structure of Ca(SCN)$_2$ · 2 H$_2$O. The chains shown in Fig. 2 are connected via the SCN$^-$ ions.

Table 3. Selected distances (pm) and angles (°) for Ca(SCN)$_2$ · 2 H$_2$O.

Ca-N1	238.9(4)	C1-N1	116.1(5)
Ca-N2	241.0(3)	C1-S1	164.6(4)
Ca-S2	308.0(1)	C2-N2	115.9(5)
Ca-S1	315.2(1)	C2-S2	164.6(4)
Ca-O (2×)	248.9(2)	O-H1	71(3)
Ca-O (2×)	257.9(2)	O-H2	77(4)
N1-C1-S1	178.8(4)	H1-O-H2	101(4)
N2-C2-S2	177.1(4)		
Hydrogen bonds			
O-S1	334.9(2)	O-S2	342.5(2)
S1-H1	271(4)	S2-H2	272(4)
O-H1-S1	151(2)	O-H2-S2	155(2)

Table 4. Atomic positions and equivalent isotropic displacement parameters (in pm^2) for Ca(SCN)$_2$.

Atom	Site	*x/a*	*y/b*	*z/c*	$U_{eq}\cdot 10^{-1}$
Ca	4*e*	1/2	0.0923(1)	3/4	12.0(2)
S1	8*f*	0.79745(8)	0.9403(1)	0.6755(1)	18.1(2)
C1	8*f*	0.6162(3)	0.3602(4)	0.3985(3)	11.8(6)
N1	8*f*	0.5565(3)	0.2148(4)	0.4496(3)	15.6(6)

$U_{eq} = {}^1/_3[U_{22} + \sin^{-2}\beta(U_{11} + U_{33} + 2\,U_{13}\cos\beta)]$ [10].

Table 5. Selected distances (pm) and angles (°) for Ca(SCN)$_2$.

Ca-N (2×)	255.8(2)	C-N	117.0(4)
Ca-N (2×)	257.6(2)	C-S	163.9(3)
Ca-S (2×)	301.7(1)		
Ca-S (2×)	308.7(1)	N-C-S	178.5(3)

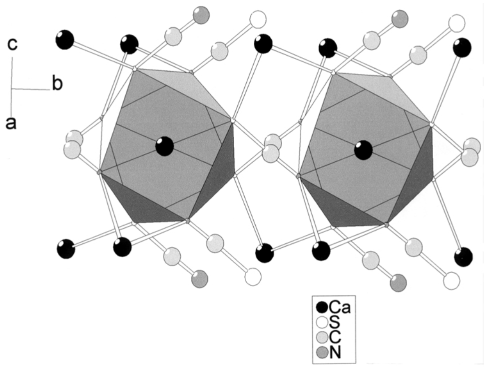

Fig. 4. Chains of the [Ca(SCN)$_8$] polyhedra in Ca(SCN)$_2$.

Ca-O distances are also similar in both compounds (Ca(SCN)$_2$ · 2 H$_2$O: 249 and 258 pm, Ca(SCN)$_2$ · 4 H$_2$O: 240 - 269 pm). The distances C-N and C-S show typical values for both SCN$^-$ ions (Table 3). One angle S-C-N (178.8°) is comparable to those in M(SCN)$_2$ (M = Eu, Ca, Sr, Ba) while the other one (177.1° for S2-C2-N2) is slightly smaller.

The [Ca(SCN)$_4$ (H$_2$O)$_4$] polyhedra are connected via common oxygen edges to chains along [010] (Fig. 2) in such a way that the respective SCN$^-$ ions are arranged opposite to those of the neighboring polyhedra. The four SCN$^-$ ions of one polyhedron are part of four different chains, resulting in a three-dimensional network. This structure can also be described to consist of layers of SCN$^-$ and Ca^{2+} ions which are connected via water molecules (Fig. 3). The hydrogen atoms of the water molecules point towards the nitrogen and the sulfur atoms of the thiocyanate groups so that S···H and N···H hydrogen bonds can be formed. While the S···H distances (271 and 272 pm) indicate strong hydrogen

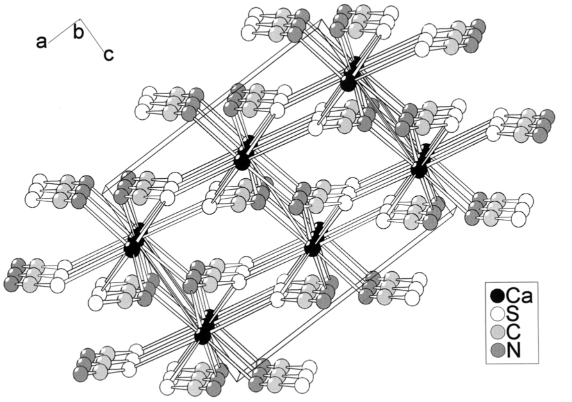

Fig. 5. Perspective view of the crystal struture of $Ca(SCN)_2$.

bonds [12] the values for the N···H distances (286 and 289 pm) are too long for significant hydrogen bonding.

$Ca(SCN)_2$ crystallizes isotypically with $M(SCN)_2$ (M = Eu, Sr, Ba [3], Pb [13]) with the monoclinic space group *C 2/c* with four formula units per cell (Table 1). Isotypism of Ca^{2+} and Ba^{2+} compounds is rather unusual due to the significantly different ionic radii of Ca^{2+} (126 pm [14]) and Ba^{2+} (156 pm [14]) for an eightfold coordination but may be explained by the softness of the SCN^- anions which provide space for small as well as large cations in the structure.

All ions occupy only one crystallographic site (Table 4). The Ca^{2+} cations are surrounded by four sulfur and four nitrogen atoms which belong to eight SCN^- ions (Fig. 4). The coordination polyhedron has the shape of a square antiprism. The Ca-N distances are 256 and 258 pm (Table 5) and thus much longer than those in $Ca(SCN)_2 \cdot 2\ H_2O$ (Table 3). On the other hand the distances Ca-S are shorter than those of all isotypic compounds as well as in the dihydrate.

The distances and angles of the SCN^- ion are comparable to those in other thiocyanates. The SCN^- ion is surrounded by four Ca^{2+} ions, therefore the compound can be described as $[M(SCN)_{4/4}(NCS)_{4/4}]$. The $[Ca(SCN)_8]$ polyhedra are connected via four common thiocyanate ions to chains along [010]. The other four ligands connect these chains with each other via nitrogen edges and sulfur vertices. Therefore, a three-dimensional network is built which can be described as alternating layers of Ca^{2+} and SCN^- ions along [101] (Fig. 5).

Table 6. Results of the thermal behavior of $Ca(SCN)_2 \cdot 4\ H_2O$ (DTA/TG data).

Reaction	T_{onset} °C	T_{end} °C	T_{max} °C	Mass loss (%) obs.	calc.
Phase transition	27.2	41.1	62.8	0	0
Melting of $Ca(SCN)_2 \cdot 4H_2O$	62.0	65.4	76.6	0	0
$Ca(SCN)_2 \cdot 4\ H_2O \rightarrow Ca(SCN)_2$	173.9	212.8	241.3	37.7	31.6
$Ca(SCN)_2 \rightarrow CaS$	408.8	418.2	436.5	70.9	71.8

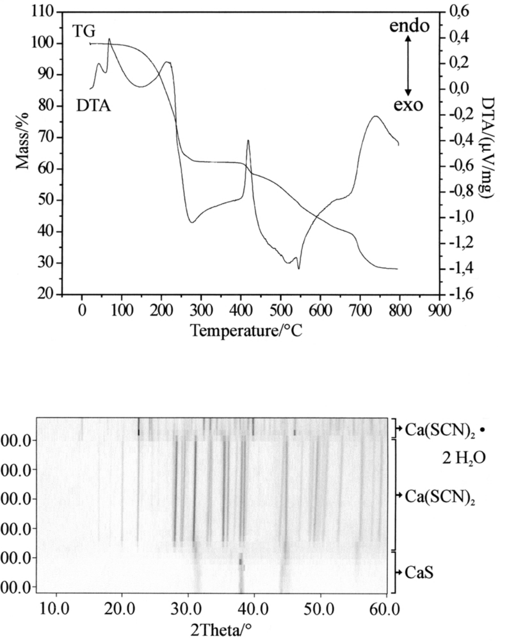

Fig. 6. DTA/TG investigations of the thermal behavior of $Ca(SCN)_2 \cdot 4H_2O$ (above). Guinier-Simon representation of the temperature dependent measurement of $Ca(SCN)_2 \cdot 2\ H_2O$ (below).

Thermal behavior

The results of the DTA/TG measurements of $Ca(SCN)_2 \cdot 4H_2O$ and the temperature dependent powder diffraction measurements of $Ca(SCN)_2 \cdot 2\ H_2O$ are shown in Fig. 6 and Table 6. The phase transition of $Ca(SCN)_2 \cdot 4\ H_2O$ is detected by an endothermic peak with an onset at 27.2 °C (Fig. 6a). The transition to the so called β form was determined in a previous investigation to occur at 23.7 °C [15]. At 62.0 °C $Ca(SCN)_2 \cdot 4\ H_2O$ begins to melt as indicated by the endothermic peak in Fig. 6a without a mass loss. At 173.9 °C the dehydration starts, but no dihydrate could be detected in

Table 7. Frequencies (in cm^{-1}) and assignements of the IR and Raman bands of $Ca(SCN)_2 \cdot 2\,H_2O$ and $Ca(SCN)_2$.

$Ca(SCN)_2 \cdot 2H_2O$ IR	$Ca(SCN)_2 \cdot 2H_2O$ Raman	$Ca(SCN)_2$ IR	$Ca(SCN)_2$ Raman	Vibration	Frequences of the free species
	72		87	outer vibrations	
	95		99		
	137		129		
			160		
	172		172		
	199		183		
	261		228		
469	440	469	477		
478	451	477	490	δ(SCN)	470(Π)
	473	481	500		[16]
	488				
515	540			?	
627	608			?	
769	768	764	777	ν(SC)	743(Σ^+)
		770			[16]
951	933	942	951		
957		958	974	2δ(SCN)	
		967	995		
1628	1628			$\delta(H_2O)$	1595(A_1) [17]
2077	2100	2013	2010		
2096	2116	2077	2029	ν(CN)	2066(Σ^+)
2123	2124		2048		[16]
	2185				
3242	3252			$\nu_s(H_2O)$	3657(A_1) [17]
3398	3360			$\nu_{as}(H_2O)$	3756(B_2) [17]

the course of the DTA measurement. The observed mass loss is 37.7% while 31.6% are theoretically expected. The difference can be explained by the assumption that some water was retained in the sample or partial decomposition occurs. For comparision, the powder diffraction measurements (Fig. 6b) show a dehydration of $Ca(SCN)_2 \cdot 2H_2O$ starting at 90 °C which is complete at 110°C, when the powder pattern can be assigned to $Ca(SCN)_2$. The difference in the observed temperatures detected by the two methods can be explained by the inaccuracy of the temperature determination of the powder method.

Both measurements have shown that $Ca(SCN)_2$ starts to decompose at about 420 °C. In the DTA curve, an endothermic peak is detected, and the TG measurements show a slow complicated decomposition. Probably $Ca(SCN)_2$ starts to melt at 408.8 °C and the decomposition starts directly after melting. According to X-ray powder measurements at 500 °C this decomposition is quantitative, and the pattern of the product can be assigned to CaS. This is in agreement with the findings for the isotypic thiocyanates $M(SCN)_2$ (M = Eu, Sr, Ba) [3]. Moreover, the starting point of the decomposition decreases from $Ba(SCN)_2$ (672 °C) to $Sr(SCN)_2$ (650 °C) and $Eu(SCN)_2$ (557 °C) [3]. The further decrease of the decomposition temperature when going to $Ca(SCN)_2$ is in accordance to this. The mass of the residue is 28.2% of the initial amount of $Ca(SCN)_2 \cdot 4\,H_2O$, indicating that CaS has formed (calculated: 31.9 %).

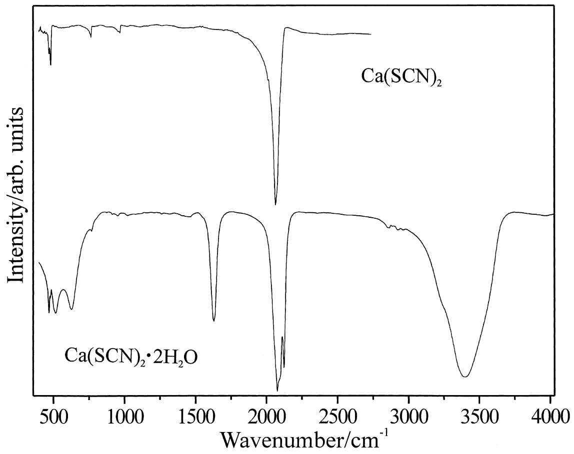

Fig. 7. IR spectra of $Ca(SCN)_2 \cdot 2\,H_2O$ and $Ca(SCN)_2$.

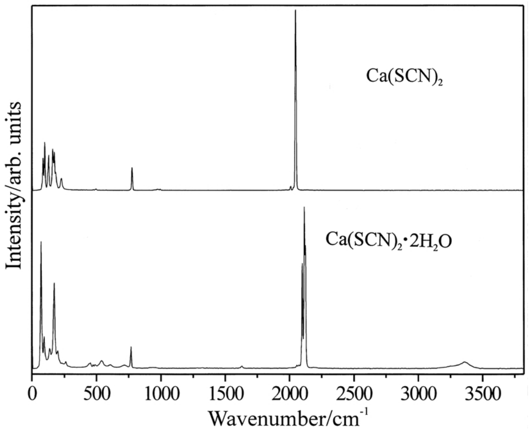

Fig. 8. Raman spectra of $Ca(SCN)_2 \cdot 2H_2O$ and $Ca(SCN)_2$.

Vibrational spectroscopy

The space group *C2/c* of $Ca(SCN)_2$ leads to the factor group C_{2h} with $Z = 2$ in the primitive unit cell. A maximum of 39 vibrations are to be expected which can be described by four different irreducible representations according to $\Gamma_v = 10\ A_g + 9\ A_u +$

$11\,B_g + 9\,B_u$. 21 vibrations of *gerade* symmetry are observable in Raman spectra, while 18 of *ungerade* symmetry can be detected in IR measurements. In our experiments, 14 and 7 vibrations were observed in the Raman and IR spectra, respectively (Table 7, Fig. 7, 8). The difference between the expected and observed IR vibrations is mainly due to the onset of the measurements at 400 cm^{-1}, excluding the vibrations at low frequencies. Besides, some vibrations may have too low intensities to be observed, or the transitions are too close in energy to be resolved. $Ca(SCN)_2 \cdot 2\,H_2O$ can be described with the factor group D_{2h} and, therefore, the optical phonon modes belong to the following irreducible representations:

$$\Gamma_v = 23\,A_g + 16\,A_u + 16\,B_{1g} + 22\,B_{1u} + 23\,B_{2g} + 15\,B_{2u} + 16\,B_{3g} + 22\,B_{3u}.$$

All modes with *gerade* symmetry are to be observed in Raman spectra while B_{1u}, B_{2u} and B_{3u} modes are IR active. Again, only a small number of these were detected due to the reasons mentioned above.

Fig. 7 and 8 show the IR and Raman spectra, respectively. The frequencies and their assignments are listed in Table 7. The transitions at low frequencies, $\nu < 300$ cm^{-1}, can be assigned to outer vibrations, *e. g.* valence vibrations like ν(MS) and ν(MN) or deformation vibrations like δ(MSC) and δ(MNC). The observed vibrations at frequencies above 400 cm^{-1} can be correlated to inner modes of the SCN^- ions or the H_2O molecules. The increasing numbers of these transitions compared to those of the free species can be due to factor group multiplication and/or to a removal of the degeneracy of modes because of the reduced symmetry in solids.

In contrast to $M(SCN)_2$ (M = Eu, Sr, Ba) where the fundamentals and the first overtones of the bending vibrations δ(SCN) could exclusivly be detected in the IR spectra [3], they are observed in the IR as well as in the Raman spectra in the present case. The two bands between 500 and 700 cm^{-1} which are found in both spectra of $Ca(SCN)_2 \cdot 2\,H_2O$ could not be assigned unambiguously. They cannot be due to valence vibrations of the hydrogen bonds because they are expected to be at lower energy for relatively weak bonds. But they may originate from librational modes of hydrogen bonded water molecules which appear because of hindered rotation. Librational vibrations are found as broad intensive bands in IR, but weak ones in Raman spectra and are positioned at 850 cm^{-1} in solid H_2O [18]. In this case they are expected to be at lower energy because of the weaker hydrogen bonds.

The stretching vibrations of the water molecule are shifted by 400 cm^{-1} to lower energy compared to free H_2O as it is expected for hydrogen bond systems [18]. On the other hand, the respective bending vibrations are blue shifted by a few percent, as it is observed in the present case. Additionally, the stretching vibrations are very broad, which is another phenomenon attributed to hydrogen bonds. Note that the present case is an illustrative example of the large intensity of stretching modes of water molecules in the IR spectra compared to Raman spectra.

The position of the modes belonging to SCN^- ions depends on the bonding conditions. In the case of N bonding δ(SCN) and ν(SC) are positioned at lower frequencies compared to the free ion, and at higher frequencies in the case of S bonding [19]. The respective frequencies of $Ca(SCN)_2$ and $Ca(SCN)_2 \cdot 2H_2O$ are similar to those of the free ion due to SCN^- bridging. On the other hand ν(NC) is expected to show values above 2100 cm^{-1} in SCN^- bridging compounds [20] which is indeed fullfiled for $Ca(SCN)_2 \cdot 2\,H_2O$. In contrast, the stretching S-C modes are at lower frequencies for the water free compound, owing to several different factors [21].

Acknowledgements

The authors are indebted to Prof. Dr. G. Meyer, Institut für Anorganische Chemie, Universität zu Köln, for generous support. The preparation of $Ca(SCN)_2 \cdot 4H_2O$ by Prof. Dr. L. Bohatý and Dr. P. Held, Institut für Kristallographie, Universität zu Köln, is gratefully acknowledged.

---

[1] G. Blasse, B. C. Grabmaier, Luminescent Materials, Springer Verlag, Berlin (1994).

[2] P. Dorenbos, submitted to Phys. Rev. B.

[3] C. Wickleder, Z. Anorg. Allg. Chem. **627**, 1693 (2001).

[4] C. Wickleder, P. Larsen, submitted to J. Lumin.

[5] P. Held, L. Bohaty, Z. Kristallogr. NCS **216**, 337 (2001).

[6] R. J. Meyer, E. H. E. Pietsch, Gmelins Handbuch der Anorganischen Chemie, 28 B, Verlag Chemie, Weinheim (1961).

[7] G. M. Sheldrick, SHELXS-86, Programs for X-ray structure analysis, Göttingen (1986); G. M. Sheldrick, SHELXL-93, Program for the Refinement of Crystal Structures, Göttingen (1993).

[8] X-RED 1.07, Data Reduction for STADI4 and IPDS, Stoe & Cie Darmstadt 1996; X-SHAPE 1.01, Crystal Optimisation for Numerical Absorption Correction, Stoe & Cie Darmstadt (1996).

[9] Th. Hahn (ed.), International Tables for Crystallography, Vol. C, D. Reidel Publishing Company, Dordrecht, Boston (1983).

[10] R. X. Fischer, E. Tillmanns, Acta Crystallogr. **C44**, 775 (1988).

[11] Netzsch GmbH, Thermal Analysis for the Analyzer STA 409, version3.1, Selb (1996).

[12] T. Steiner, Angew. Chem. **114**, 50 (2002).

[13] J. A. A. Mokuolu, J. C. Speakman, Acta Crystallogr. **B31**, 172 (1975).

[14] R. D. Shannon, C. T. Prettwitt, Acta Crystallogr. **B25**, 925 (1969); R. D. Shannon, Acta Crystallogr. **A32**, 751 (1976).

[15] A. K. McKerrow, V. J. Occleshaw, F. Grabble, J. Chem. Soc. 5 (1946).

[16] L. H. Jones, J. Chem. Phys. **25,** 1069 (1956); L. H. Jones, J. Chem. Phys. **28**, 1234 (1958).

[17] W. S. Benedict, N. Gailar, E. K. Plyler, J. Chem. Phys. **24,** 1139 (1956).

[18] H. Siebert, Anwendungen der Schwingungsspektroskopie in der Anorganischen Chemie, Springer Verlag, Berlin (1966).

[19] W. Preetz, U. Horns, Z. Anorg. Allg. Chem. **516**, 159 (1984); O. Stähler, W. Preetz, Z. Anorg. Allg. Chem. **626**, 2077 (2000).

[20] P. C. H. Mitchell, R. J. P. Williams, J. Chem. Soc. 1912 (1960).

[21] R. A. Bailey, S. L. Kozak, T. W. Michelsen, W. N. Mills, Coord. Chem. Rev. **6**, 407 (1971).